

**AFRL-VA-WP-TP-2002-323**

**APPROXIMATE METHODS FOR  
CENTER OF PRESSURE PREDICTION  
OF MULTI-SEGMENT WINGS**



**Sarah C. Blackmar  
Mark S. Miller  
William B. Blake**

**OCTOBER 2002**

**Approved for public release; distribution is unlimited.**

**©2002 AIAA**

**This work is copyrighted. The United States has for itself and others acting on its behalf an unlimited, paid-up, nonexclusive, irrevocable worldwide license. Any other form of use is subject to copyright restrictions.**

**20021212 139**

**AIR VEHICLES DIRECTORATE  
AIR FORCE RESEARCH LABORATORY  
AIR FORCE MATERIEL COMMAND  
WRIGHT-PATTERSON AIR FORCE BASE, OH 45433-7542**

<b>REPORT DOCUMENTATION PAGE</b>				<i>Form Approved</i> OMB No. 0704-0188	
The public reporting burden for this collection of information is estimated to average 1 hour per response, including the time for reviewing instructions, searching existing data sources, gathering and maintaining the data needed, and completing and reviewing the collection of information. Send comments regarding this burden estimate or any other aspect of this collection of information, including suggestions for reducing this burden, to Department of Defense, Washington Headquarters Services, Directorate for Information Operations and Reports (0704-0188), 1215 Jefferson Davis Highway, Suite 1204, Arlington, VA 22202-4302. Respondents should be aware that notwithstanding any other provision of law, no person shall be subject to any penalty for failing to comply with a collection of information if it does not display a currently valid OMB control number. <b>PLEASE DO NOT RETURN YOUR FORM TO THE ABOVE ADDRESS.</b>					
<b>1. REPORT DATE (DD-MM-YY)</b> October 2002		<b>2. REPORT TYPE</b> Conference Paper		<b>3. DATES COVERED (From - To)</b>	
<b>4. TITLE AND SUBTITLE</b> APPROXIMATE METHODS FOR CENTER OF PRESSURE PREDICTION OF MULTI-SEGMENT WINGS				<b>5a. CONTRACT NUMBER</b> GS-23-F-0103K	
				<b>5b. GRANT NUMBER</b>	
				<b>5c. PROGRAM ELEMENT NUMBER</b> 62201F	
<b>6. AUTHOR(S)</b> Sarah C. Blackmar and Mark S. Miller (Dynetics, Inc.) William B. Blake (AFRL/VACA)				<b>5d. PROJECT NUMBER</b> N/A	
				<b>5e. TASK NUMBER</b> N/A	
				<b>5f. WORK UNIT NUMBER</b> N/A	
<b>7. PERFORMING ORGANIZATION NAME(S) AND ADDRESS(ES)</b> <div style="display: flex; justify-content: space-between;"> <div style="width: 45%;">           Dynetics, Inc.            1000 Explorer Blvd NW            Huntsville, AL 35806         </div> <div style="width: 50%;">           Control Theory Optimization Branch (AFRL/VACA)            Control Sciences Division            Air Vehicles Directorate            Air Force Research Laboratory, Air Force Materiel Command            Wright-Patterson Air Force Base, OH 45433-7542         </div> </div>				<b>8. PERFORMING ORGANIZATION REPORT NUMBER</b>	
<b>9. SPONSORING/MONITORING AGENCY NAME(S) AND ADDRESS(ES)</b> Air Vehicles Directorate Air Force Research Laboratory Air Force Materiel Command Wright-Patterson Air Force Base, OH 45433-7542				<b>10. SPONSORING/MONITORING AGENCY ACRONYM(S)</b> AFRL/VACA	
				<b>11. SPONSORING/MONITORING AGENCY REPORT NUMBER(S)</b> AFRL-VA-WP-TP-2002-323	
<b>12. DISTRIBUTION/AVAILABILITY STATEMENT</b> Approved for public release; distribution is unlimited.					
<b>13. SUPPLEMENTARY NOTES</b> AIAA Applied Aerodynamics Conference presentation, Orlando, FL, June 2003. ©2002 AIAA. This work is copyrighted. The United States has for itself and others acting on its behalf an unlimited, paid-up, nonexclusive, irrevocable worldwide license. Any other form of use is subject to copyright restrictions.					
<b>14. ABSTRACT (Maximum 200 Words)</b> Approximate methods for predicting the center of pressure of multi-segment wings are presented. Only wings with breaks in the leading edge sweep are considered. The methods transform a multi-segment planform into an equivalent straight tapered planform. Comparisons are made with predictions from a vortex lattice code and experimental data at subsonic speeds and with predictions from a vortex lattice and an Euler code at supersonic speeds. The most accurate method studied had an average error in predicted center of pressure location of approximately 2 percent of the root chord.					
<b>15. SUBJECT TERMS</b> Aerodynamics, center of pressure					
<b>16. SECURITY CLASSIFICATION OF:</b>			<b>17. LIMITATION OF ABSTRACT:</b> SAR	<b>18. NUMBER OF PAGES</b> 18	<b>19a. NAME OF RESPONSIBLE PERSON (Monitor)</b> William B. Blake <b>19b. TELEPHONE NUMBER (Include Area Code)</b> (937) 255-6764
<b>a. REPORT</b> Unclassified	<b>b. ABSTRACT</b> Unclassified	<b>c. THIS PAGE</b> Unclassified			

# Approximate Methods for Center of Pressure Prediction of Multi-Segment Wings

Sarah C. Blackmar\* and Mark S. Miller\*\*

*Dynetics, Inc.  
Huntsville, Alabama*

William B. Blake\*\*

*Air Force Research Laboratory, Air Vehicles Directorate  
Wright Patterson Air Force Base, Ohio*

## ABSTRACT

Approximate methods for predicting the center of pressure of multi-segment wings are presented. Only wings with breaks in the leading edge sweep are considered. The methods transform a multi-segment planform into an equivalent straight tapered planform. Comparisons are made with predictions from a vortex lattice code and experimental data at subsonic speeds and with predictions from a vortex lattice and an Euler code at supersonic speeds. The most accurate method studied had an average error in predicted center of pressure location of approximately two percent of the root chord.

## LIST OF SYMBOLS

$\alpha$	angle of attack
AR	aspect ratio, $b^2/S$
$b$	wing span
$C_m$	pitching moment coef., (pitching moment/ $q_\infty S c_r$ )
$C_N$	normal force coef., (normal force/ $q_\infty S$ )
$c_r$	root chord
$c_t$	tip chord
$\Lambda$	sweep angle
$\eta$	lateral position of break in sweep angle, $y/(b/2)$
$\lambda$	taper ratio ( $c_r/c_t$ )
$q_\infty$	dynamic pressure
RN	Reynold's number
$S$	wing area
$x_{cp}$	center of pressure, measured aft of apex
XCP	center of pressure, measured aft of apex, $x_{cp}$
$x_{cent}$	area centroid, measured aft of apex

### Subscripts

LE	leading edge
TE	trailing edge

\* Member, AIAA

\*\* Associate Fellow, AIAA

## INTRODUCTION

Typical tactical missiles have fins with small chord lengths relative to the overall body length. As a result, static stability and trim are not significantly affected by errors in the predicted center of pressure of these fins. Many high-speed vehicles, however, employ very highly swept strakes on the inboard portion of the wing. In some cases, the strakes are so large that the root chord of the wing is as long as the fuselage. The stability and trim of these configurations are much more sensitive to errors in the predicted wing center of pressure.

Preliminary aerodynamic design codes such as Missile Datcom (Ref. 1) and the Naval Surface Warfare Center AP98 (Ref. 2) use approximate methods to model straked wings. Given a straked wing geometry, they define an equivalent straight tapered wing which is used for the subsequent analysis. Spencer (Ref. 3) showed that the equivalent wing method can produce excellent subsonic lift predictions if the appropriate algorithm is used to define the equivalent straight tapered wing. However, he did not extend his analysis to include supersonic speeds or consider center of pressure predictions.

The algorithm used for multi-segment wing center of pressure ( $x_{cp}$ ) calculations in the 8/99 version of Missile Datcom has been found to be inadequate when compared with data from future generation reusable launch vehicles with long strakes such as the X-34 and X-37 shown in Figure 1. The objective of this effort was to identify an alternative transformation methodology for yielding improved  $x_{cp}$  predictions for multi-segment wings at small angles of attack suitable for inclusion into a future release of Missile Datcom. Only planforms with a break in the leading edge sweep were considered. Planforms with breaks in the trailing edge will be studied in a subsequent effort.

## TECHNICAL APPROACH

The problem of developing an algorithm for multi-segment wing center of pressure calculations can be divided into two distinct parts: (1) defining the equivalent planform geometry and (2) placing the center of pressure determined from the equivalent planform onto the actual planform. For this study, nine methods for defining the equivalent planform geometry were analyzed and three methods for placing the center of pressure onto the segmented planform were considered. Details concerning each of the methods evaluated as part of this investigation are presented next followed by a discussion of the approach used for their evaluation.

### Transformation Methods

Missile Datcom computes the center of pressure of a wing using design charts which are a function of aspect ratio, taper ratio, leading edge sweep angle and Mach number. All of the transformation methods investigated held constant the total area ( $S$ ), span ( $b/2$ ), and aspect ratio ( $AR$ ) of the original planform, while allowing other aspects of the wing geometry to vary. For purposes of convenience and comparison, the equations used for each of the transformation methods are provided in Table 1. A more formal derivation of these equations follows.

#### Method A

The wing transformation approach used for center of pressure calculations at all speeds in the 8/99 version of Missile Datcom is denoted as Method A. Missile Datcom also uses this method to compute the normal force slope of multi-segment wings at supersonic speeds. The method evaluates a segmented planform by transforming the planform into a straight-tapered approximation with the same taper ratio as the original planform and defines an effective leading edge sweep angle based on the area-weighted average of the leading edge sweep angles of each segment, using:

$$\Lambda_{LE} = \frac{1}{S} [\sum \Lambda_{LE,i} S_i] \quad (1)$$

where ( $\Lambda_{LE,i}$ ) and  $S_i$  define the leading edge sweep angle and planform area of each wing segment, respectively. The root chord of the transformed wing is calculated using:

$$c_r = \frac{2S}{b(1+\lambda)} \quad (2)$$

Method A calculates the  $x_{cp}$  of the transformed wing using a proportional method that preserves the location of the  $x_{cp}$  as a percentage of the root chord as follows:

$$\left( \frac{x_{cp}}{c_r} \right) = \left( \frac{x_{cp}}{c_r} \right)_{effective} \quad (3)$$

#### Method B

Method B uses the transformation developed by Spencer for wings at subsonic speeds, Ref. 3. Missile Datcom uses this method to compute the normal force slope of multi-segment wings at subsonic speeds. It computes an effective mid-chord sweep angle ( $\Lambda_{c/2}$ ) using an area-weighted average:

$$\Lambda_{c/2} = \cos^{-1} \left[ \frac{1}{S} \sum \cos \Lambda_{c/2,i} S_i \right] \quad (4)$$

This is then used to calculate the effective leading edge sweep angle using:

$$\Lambda_{LE} = \tan^{-1} \left[ \tan \Lambda_{c/2} + \frac{2(1-\lambda)}{AR(1+\lambda)} \right] \quad (5)$$

Like Method A, Method B maintains the taper ratio of the original wing and uses the proportional placement approach provided by Equation 3 to translate the  $x_{cp}$  of the transformed fin onto the original fin.

#### Method C

Method C is a variation of Method B that uses the mid-chord sweep angle rather than the cosine of the angle to calculate the effective sweep:

$$\Lambda_{c/2} = \frac{1}{S} \sum \Lambda_{c/2,i} S_i \quad (6)$$

Like the two preceding methods, this method maintains the taper ratio of the original wing and locates the  $x_{cp}$  of the segmented planform proportionally according to Equation 3.

#### Method D

Method D (Ref. 4) differs significantly from the previous methods in that it holds constant the trailing edge sweep angle and tip chord of the original planform to define a straight-tapered panel, and allows the taper ratio to vary.

The effective leading edge sweep angle based on the trailing edge sweep, aspect ratio, and taper ratio of the original planform is calculated using:

$$\Lambda_{LE} = \tan^{-1} \left[ \tan \Lambda_{TE} + \frac{4}{AR} \frac{(1-\lambda)}{(1+\lambda)} \right] \quad (7)$$

The effective root chord of the planform is computed using:

$$c_r = \frac{2S}{b} - c_t \quad (8)$$

This method also uses a different procedure to translate the  $x_{cp}$  of the transformed wing back onto the original planform. Rather than placing the  $x_{cp}$  proportionally, as the previous methods do, Method D lines up the trailing edges of the segmented and straight-tapered planforms, and places the  $x_{cp}$  of the original planform at the same distance from the trailing edge as the  $x_{cp}$  of the transformed planform. This realignment of the  $x_{cp}$  from the transformed wing to the original wing can be performed using:

$$\left( \frac{x_{cp}}{c_r} \right) = 1 - \left[ 1 - \left( \frac{x_{cp}}{c_r} \right)_{effective} \right] \frac{c_{r,effective}}{c_r} \quad (9)$$

#### Method E

Method E is a variation of Method D that maintains the taper ratio of the original planform rather than the tip chord. It also uses the same aft  $x_{cp}$  trailing edge alignment method as Method D (Equation 9).

Both Methods D and E could be extended to planforms with breaks in the trailing edge sweep angle by using:

$$\Lambda_{TE} = \frac{1}{S} \sum \Lambda_{TE,i} S_i \quad (10)$$

#### Method F

A hybrid method, denoted as Method F, combines approaches used in Methods A and D. Like Method A, this method uses Equation 1 to calculate an effective leading edge sweep angle and uses the proportional placement approach defined in Equation 2 for locating  $x_{cp}$ . However, the tip chord of the original planform is held constant, as is done for Method D.

#### Method G

The equivalent tangent leading edge sweep method, denoted as Method G, maintains the same geometric properties and uses the same  $x_{cp}$  placement method as Method A; however, it uses the tangents of the segmented wing leading edge sweep angles to determine an effective leading edge sweep angle using:

$$\Lambda_{LE} = \tan^{-1} \left[ \frac{1}{S} \sum \tan \Lambda_{LE,i} S_i \right] \quad (11)$$

#### Method H

Method H, obtained from Reference 2, is one of two wing transformation methods contained the AP98 aerodynamic prediction code. The method holds constant both the inboard leading edge sweep angle and the trailing edge sweep angle of the original planform, and uses the equations below to calculate new root and tip chords, respectively.

$$c_r = \left[ \frac{S}{b} - \frac{b}{4} (\tan \Lambda_{TE} - \tan \Lambda_{LE}) \right] \quad (12)$$

$$c_t = \left[ \frac{S}{b} + \frac{b}{4} (\tan \Lambda_{TE} - \tan \Lambda_{LE}) \right] \quad (13)$$

For configurations where the inboard section of the wing is highly swept, such as with strakes, these equations can yield negative tip chords. This method was not evaluated where a negative value for tip chord was obtained in this study. However, AP98 assigns a tip chord of zero and calculates a new root chord in these cases.

The  $x_{cp}$  placement approach that AP98 uses lines up the area centroids of the original and transformed wings and places the  $x_{cp}$  of the segmented wing the same distance from the centroid as is the  $x_{cp}$  of the straight-tapered wing, using:

$$\left( \frac{x_{cp}}{c_r} \right) = \left( \frac{x_{cent}}{c_r} \right) + \frac{c_{r,effective}}{c_r} \left( \frac{x_{cp} - x_{cent}}{c_r} \right)_{effective} \quad (14)$$

#### Method I

The second method used by AP98, denoted as Method I, maintains the inboard leading edge sweep angle of the

original planform as is done for Method H. However, Method I maintains the taper ratio of the original planform and allows the trailing edge sweep angle to vary. It uses the area centroid placement approach used by Method H to locate the  $x_{cp}$  of the segmented wing.

### Evaluation Approach

An extensive literature search was performed to locate experimental data suitable for further evaluation and validation of the most promising wing transformation approaches. Unfortunately, very little data for isolated wings is available, and what little was identified exists only at subsonic speeds. In order to perform as systematic evaluation of the accuracy of the various transformation methods, fourteen segmented planforms were defined to represent a broad range of reusable launch vehicle and missile fin designs. Referring to Figure 2, the wing geometric parameters varied for this study included: inboard and outboard leading edge sweep angle, trailing edge sweep angle, taper ratio, and spanwise location of the sweep break. The span of the planforms was held constant. Table 2 lists the design parameters of the segmented planforms investigated. Corresponding scaled drawings of these wings are provided in Figure 3.

Each of the segmented planform designs was converted into equivalent straight tapered planforms using the nine wing transformation methods previously described. These configurations were analyzed with Missile Datcom at Mach numbers of 0.3, 2.0, and 4.0 to obtain a set of  $C_m$  and  $C_N$  predictions from which an  $x_{cp}$  prediction (defined in terms of root chord percentage) was calculated as:

$$\frac{x_{cp}}{c_r} = -\frac{C_m}{C_N} \quad (@ \alpha = 4 \text{ deg}) \quad (15)$$

In order to determine which of the methods examined was most accurate, comparisons were made between Missile Datcom results, obtained on each of the transformed straight tapered planforms, and "exact" analytical solutions, obtained for each original multi-segmented using the vortex lattice code HASC (Reference). The HASC analysis was performed at the same Mach numbers and angles of attack as the Missile Datcom analysis. The Missile Datcom results for all of the transformed wings assumed proportional placement for  $x_{cp}$  (Eq. 3). These were post-processed to give trailing edge placement for Methods D and E and centroid placement for Methods H and I.

To address numerical uncertainty issues associated with the placement and density of the bound vortices modeled

in HASC, a parametric sensitivity study was performed by varying the number of chordwise and spanwise bound vortices for a limited set of both multi-sweep and straight-tapered wing geometries for which experimental data were available. Results from this study were used as a guide for the vortex distributions applied on each of the fourteen multi-segmented planforms evaluated. The distributions used for assessing the Missile Datcom results were sufficient to limit numeric difference associated with the vortex distributions to less than 0.1% of the calculated  $x_{cp}/c_r$  value.

As an additional check of the validity of using HASC to perform this evaluation, three of the multi-segment planforms (Configurations 1, 3, and 13) were analyzed using the space-marching Euler code ZEUS (Ref. 6). These results were compared with the HASC results for  $x_{cp}/c_r$  at Mach 2 and 4 and found to be within 1 percent of one another at a four-degree angle of attack.

All predicted results obtained for this investigation (Missile Datcom, HASC, and ZEUS) were independent of Reynold's number and assumed infinitely thin cross sections. Sign conventions used for the analysis are shown in Figure 4.

### RESULTS AND ANALYSIS

Table 3 provides a summary of the average error in center of pressure location, as a fraction of the root chord length, for each of the nine methods considered at Mach 0.3, 2.0 and 4.0. The percent error is defined as the percent difference between the results obtained using the various transformation methods and the "exact" analytical solutions obtained from HASC. Methods D and E are clearly superior to the other methods with average errors on the order of 1/4 or less of those obtained using the transformation method used in the 8/99 version of Missile Datcom (Method A). With only one exception, all of the methods investigated provided greater accuracy than Method A. As noted above, the data reduction procedure generated proportional  $x_{cp}$  placement results for the planforms generated by Methods D, E, H and I. These were inferior to the desired placement results in all cases.

Figure 5 plots the percent error in wing  $x_{cp}$  versus wing aspect ratio for each of the 14 segmented wings investigated at Mach 0.3, 2.0 and 4.0, respectively. In addition to the results obtained from Method A, results for Methods B, C, D and E are also included. The number of methods shown on these figures was limited to the most promising transformation approaches, in order to facilitate clear comparisons between them.

Inspection of Figure 4 shows that the errors associated with Method A are frequently greater than 10 percent at Mach 0.3 and 2.0 for wing aspect ratios less than 1.2. Methods D and E have the lowest percent errors and yield very similar results for all configurations. With the exception of the lowest aspect ratio wings (configurations 10 and 11), the  $x_{cp}$  percent error for Methods D and E is less than 5 percent for all wings at both Mach 0.3 and 2.0. The close agreement in results is not surprising given the similarity of the two methods. At Mach 4.0, all methods demonstrated greater accuracy, but the overall trends observed remained consistent with those observed at Mach 0.3 and 2.0. The  $x_{cp}$  percent error for Methods D and E were both less than 5 percent for all configurations evaluated at Mach 4.0.

Methods A and E were compared with a limited set of subsonic experimental data obtained References 7 through 11 to validate the assessments made from comparisons with "exact" solutions generated by HASC. Table 4 identifies the wing configurations and test conditions for which subsonic experimental data was obtained for validation purposes. Figure 6 provides the scaled planform views of each of the wings identified in Table 4. A plot comparing  $x_{cp}$  percent error as a function of aspect ratio for both Methods A and E is shown in Figure 7. As observed in "exact" data comparisons made in Figure 5, Method E  $x_{cp}$  predictions are consistently within five percent of the experimental data, while Method A  $x_{cp}$  errors are anywhere from two to five times greater than Method E. The maximum error for the experimental  $x_{cp}$  data is estimated to be within one percent of the wing root chord.

The values of center of pressure discussed thus far are only used by Missile Datcom for the linear lift contribution, i.e., at low angles of attack. Missile Datcom uses the wing centroid as the center of pressure for the non-linear lift contribution. The overall wing  $x_{cp}$  is computed using:

$$\frac{x_{cp}}{c_r} = \frac{C_{N,linear}(x_{cp}/c_r) + C_{N,non-linear}(x_{cent}/c_r)}{C_N} \quad (16)$$

To assess the performance of Method E relative to Method A in Missile Datcom, plots of  $x_{cp}/c_r$  were generated versus angle of attack for wing configurations 15, 16, 17, 22 and 23. These plots are presented in Figures 8 through 12 in numeric order. Method E yields significantly better yields results than Method A for all four configurations and Method E is within four percent

of experimental  $x_{cp}/c_r$  values for angles of attack up to 25 degrees.

## SUMMARY AND CONCLUSIONS

The results of this study have shown that several transformation methods are superior to the method contained in the 8/99 version of Missile Datcom. The independent validation of findings from the "exact" solutions study, obtained through the use of experimental data, has confirmed that the incorporation of Method E into Missile Datcom will result in significant improvements to the capability of the code to predict the  $x_{cp}$  of multi-segmented wings at subsonic speeds. It is also reasonable to assume that, based on the results of the "exact" study, Method E will also yield significant improvements for supersonic predictions.

Due to the inability to predict "exact" analytical solutions and the lack of experimental data, no conclusions can be drawn for the transonic flight regime. There is clearly a need to obtain experimental data for validating Method E at supersonic transonic speeds.

The next release of Missile Datcom (Version 9/02) will incorporate Method E for predicting the  $x_{cp}$  of multi-segmented wings. This improvement will be of particular benefit for the aerodynamic assessment of reusable launch vehicle design concepts as well as unconventional missile fin designs.

## ACKNOWLEDGEMENTS

A portion of this work was performed by Dynetics, Inc. under contract GS-23-F-0103K to the U.S. Air Force Research Laboratory, Air Vehicles Directorate as part of an effort to enhance the capabilities of the Missile Datcom aerodynamic prediction code.

## REFERENCES

1. Vukelich, S.R., Stoy, S.L., Burns, K.A., Castillo, J.A., and Moore, M.E., "Missile Datcom Volume 1 - Final Report," AFWAL-TR-86-3091.
2. Hymer, T.C., Moore, F.G., and Downs, C., "User's Guide for an Interactive Personal Computer Interface for the 1998 Aeroprediction Code (AP98)", NSWCDD-TR-98/7, June 1998.
3. Spencer, B., Jr., "A Simplified Method for Estimating Subsonic Lift-Curve Slope at Low Angles of Attack for Irregular Planform Wings," NASA TM X-525,

May 1961.

4. Don Isaacs private communication (need to better define)

5. Albright, A.E., Dixon, C.J., and Hegedus, M.C., "Modification and Validation of Conceptual Design Aerodynamic Prediction Method HASC95 with VTXCHN", NASA CR 4712, March 1996.

6. Wardlaw, A.B. Jr, and Davis, S.F., "A Second Order Gudonov Method for Tactical Missiles," NSWC TR 86-506, December 1986.

7. Gatlin, G.M., and McGrath, B.E., "Low-Speed Longitudinal Aerodynamic Characteristics Through Poststall for Twenty-One Novel Planform Shapes," NASA TP 3503, August 1995.

8. Spencer, B., Jr., "An Investigation at Subsonic Speeds of Aerodynamic Characteristics at Angles of Attack from -4 to 100 of a Delta Wing Reentry Configuration Having Folding Wingtip Panels," NASA TM X-288, May 1960.

9. Henderson, W.P., and Hammond, A.D., "Low-Speed Investigation of High-Lift and Lateral Control Devices on a Semispan Variable-Sweep Wing Having an Outboard Pivot Location," NASA TMX-542, May 1961.

10. den Boer, R.G. and Cunningham, A.M., "Low-Speed Unsteady Aerodynamics of a Pitching Straked Wing at High Incidence - Part I: Test Program," Journal of Aircraft, Vol 27, No. 1, January 1990, pp. 23-30.

11. Lamar, J., "Analysis and Design of Strake-Wing Configurations," Journal of Aircraft, Vol. 17, No 1., January 1980, pp. 20-27.

Table 1. Summary of Transformation Methods for Multi-Segment Wings

Method	Maintains	$\Lambda_{LE}$	$c_r$
A (Ref 1)	b, S, $\lambda$	$\frac{1}{S} \sum \Lambda_{LE,i} S_i$	$\frac{2S}{b(1+\lambda)}$
B (Ref 3)	b, S, $\lambda$	$\tan^{-1} \left[ \tan \Lambda_{c/2} + \frac{2(1-\lambda)}{AR(1+\lambda)} \right], \cos \Lambda_{c/2} = \frac{1}{S} \sum \cos \Lambda_{c/2,i} S_i$	$\frac{2S}{b(1+\lambda)}$
C	b, S, $\lambda$	$\tan^{-1} \left[ \tan \Lambda_{c/2} + \frac{2(1-\lambda)}{AR(1+\lambda)} \right], \Lambda_{c/2} = \frac{1}{S} \sum \Lambda_{c/2,i} S_i$	$\frac{2S}{b(1+\lambda)}$
D (Ref 4)	b, S, $\Lambda_{TE}, C_T$	$\tan^{-1} \left[ \tan \Lambda_{TE} + \frac{4(1-\lambda)}{AR(1+\lambda)} \right]$	$\frac{2S}{b} - C_T$
E	b, S, $\Lambda_{TE} \lambda$	$\tan^{-1} \left[ \tan \Lambda_{TE} + \frac{4(1-\lambda)}{AR(1+\lambda)} \right]$	$\frac{2S}{b(1+\lambda)}$
F	b, S, $C_T$	$\frac{1}{S} \sum \Lambda_{LE,i} S_i$	$\frac{2S}{b} - C_T$
G	b, S, $\lambda$	$\tan^{-1} \left[ \frac{1}{S} \sum \tan \Lambda_{LE,i} S_i \right]$	$\frac{2S}{b(1+\lambda)}$
H (Ref 2)	b, S, $\Lambda_{LE,1}, \Lambda_{TE,1}$	$\Lambda_{LE,1}$	$\frac{2S}{b(1+\lambda)}$
I (Ref 2)	b, S, $\Lambda_{LE,1} \lambda$	$\Lambda_{LE,1}$	$\frac{S}{b} - \frac{b}{4} (\tan \Lambda_{TE} - \tan \Lambda_{LE})$

Table 2. Fin Geometries for Systematic Investigation

Fin	$\Lambda_{LE,1}$	$\Lambda_{LE,2}$	$\Lambda_{TE}$	$\lambda$	$\eta$	AR
1	80	0	0	0.25	0.5	1.22
2	80	40	-40	0.25	0.5	0.72
3	80	40	-20	0.25	0.5	0.84
4	80	40	0	0.25	0.5	0.94
5	80	40	20	0.25	0.5	1.10
6	80	40	40	0.25	0.5	1.42
7	80	40	-20	0.25	0.25	1.28
8	80	40	0	0.25	0.25	1.60
9	80	40	20	0.25	0.25	2.1
10	80	40	0	0.25	0.5	0.56
11	0	80	0	0.5	0.5	0.40
12	40	0	0	0.5	0.5	3.82
13	0	40	0	0.5	0.5	2.72
14	0	40	0	0.25	0.25	3.32

Table 3. Average Error in Predicted  $x_{cp}$ 

Method	M = 0.3	M = 2.0	M = 4.0
A	12.2	11.0	7.5
B	5.9	6.0	3.3
C	8.6	7.8	4.2
D	2.6	3.3	1.8
E	2.3	2.8	1.1
F	8.2	8.1	6.0
G	13.5	12.3	13.3
H	9.5	9.6	6.0
I	7.7	9.3	6.0

Table 4. Fin Geometries Used for Validation

Fin	$\Lambda_{LE,1}$	$\Lambda_{LE,2}$	$\Lambda_{TE}$	$\lambda$	$\eta$	AR	Mach	RN (ft <sup>-1</sup> )	Ref.
15	80	30	-30	0	0.17	3.08	0.14	$1.0 \times 10^6$	7
16	80	40	-40	0	0.17	2.16	0.14	$1.0 \times 10^6$	7
17	70	47.5	-47.5	0	0.39	1.64	0.14	$1.0 \times 10^6$	7
18	73	47.2	0	0	0.56	1.76	0.40	$2.5 \times 10^6$	8
19	73	47	0	0.29	0.56	1.6	0.40	$2.5 \times 10^6$	8
20	73	0	0	0.29	0.56	1.76	0.40	$2.5 \times 10^6$	8
21	60	25	2	0.09	0.38	5.10	0.50	$0.9 \times 10^6$	9
22	76	40	0	0.15	0.26	2.42	0.23	$1.7 \times 10^6$	10
23	80	65	0	0	0.37	1.60	<0.2	-	11

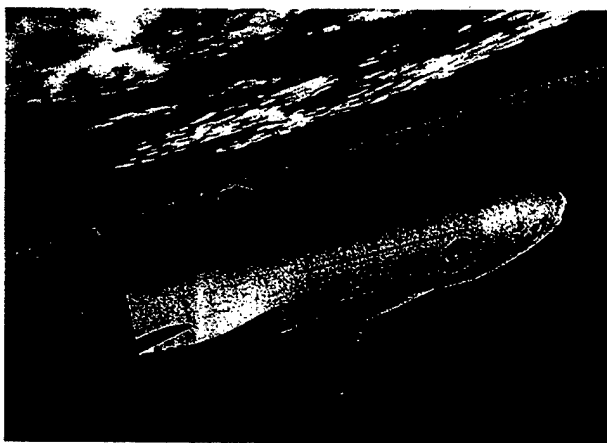
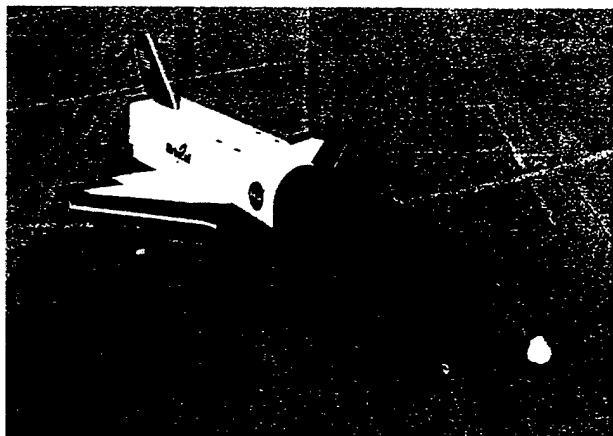


Figure 1. Photographs of X-34 and X-37.

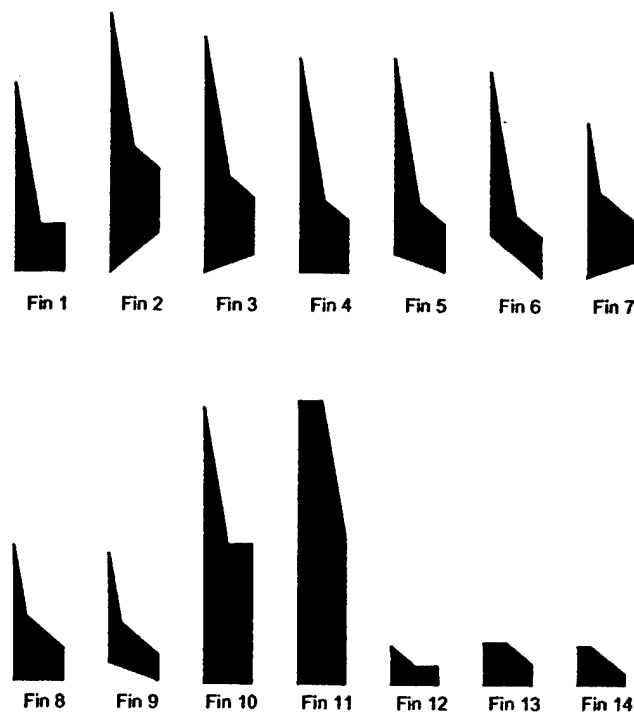


Figure 3. Wing Planforms Used for Analytic Study.

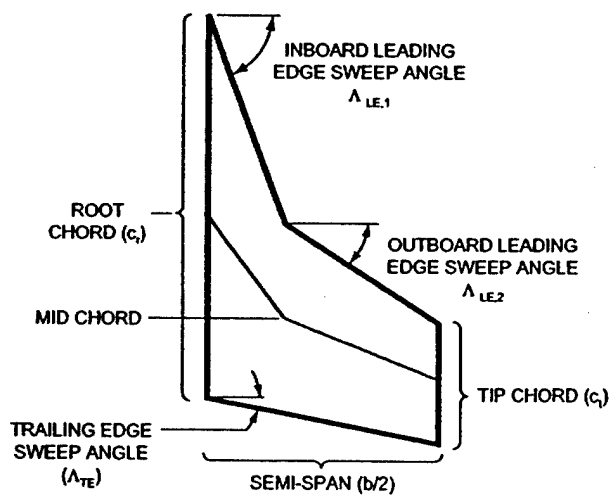


Figure 2. Wing Parameters.

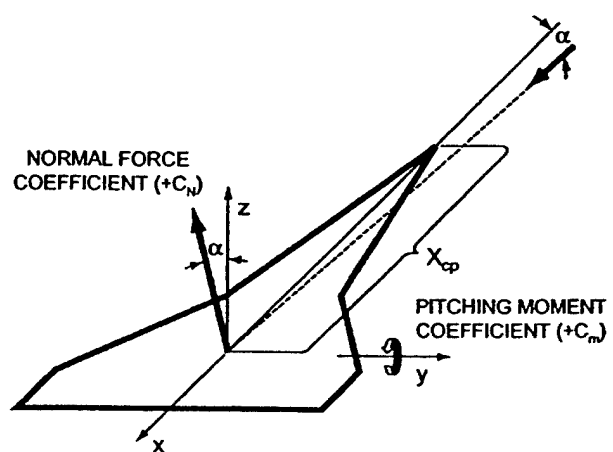


Figure 4. Sign Conventions.

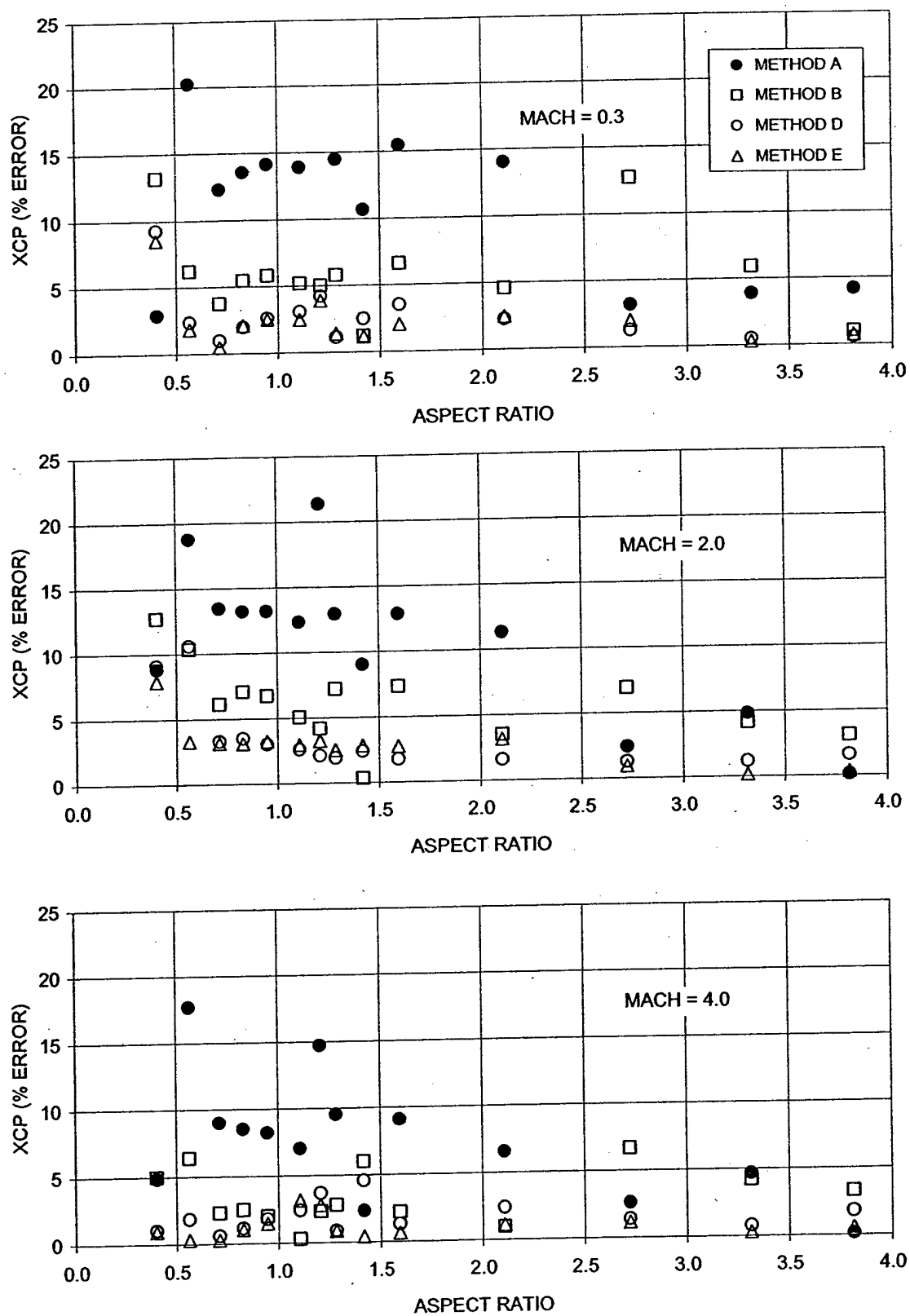


Figure 5. Analytical Error Versus Aspect Ratio.

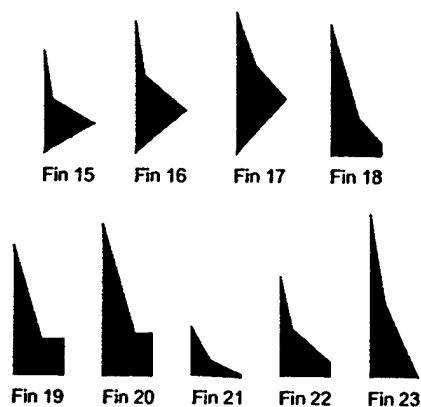


Figure 6. Wing Planforms Used for Validation.

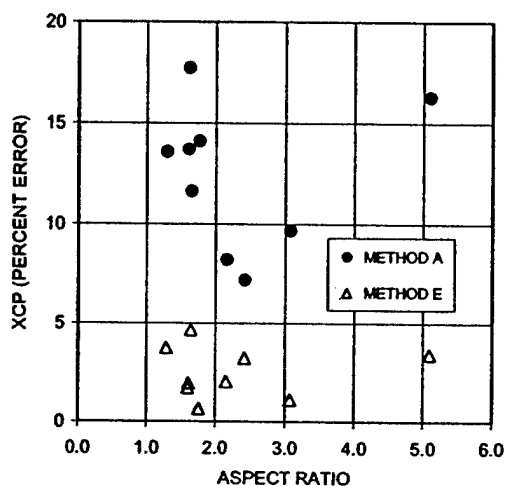


Figure 7. Experimental Error Versus Aspect Ratio.

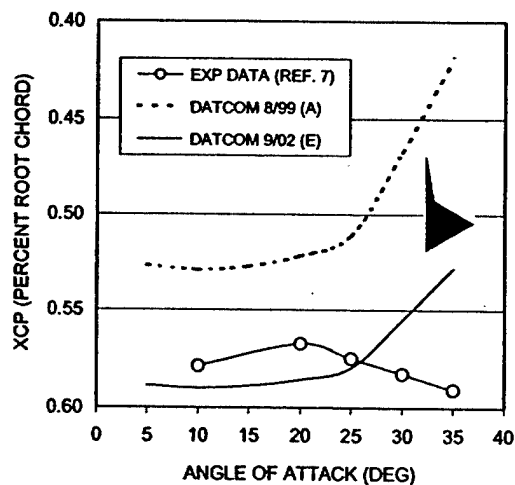


Figure 8. Wing  $x_{cp}$  Versus Angle of Attack, Configuration 15, Mach = 0.14.

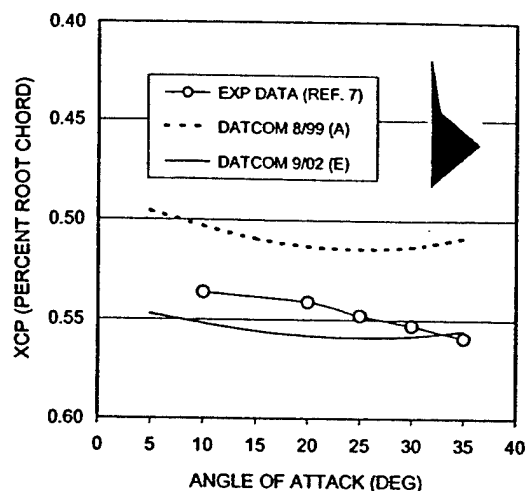


Figure 9. Wing  $x_{cp}$  Versus Angle of Attack, Configuration 16, Mach = 0.14.

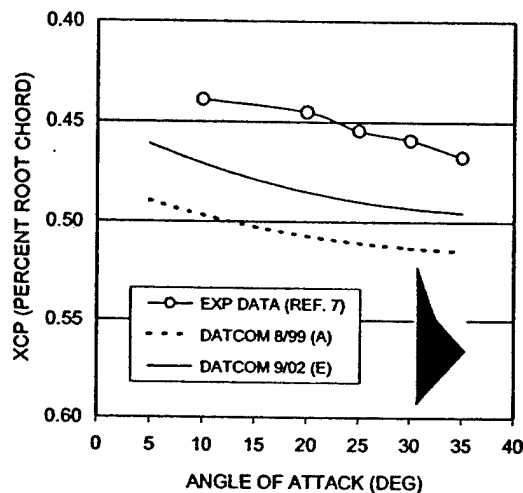


Figure 10. Wing  $x_{cp}$  Versus Angle of Attack, Configuration 17, Mach = 0.14.

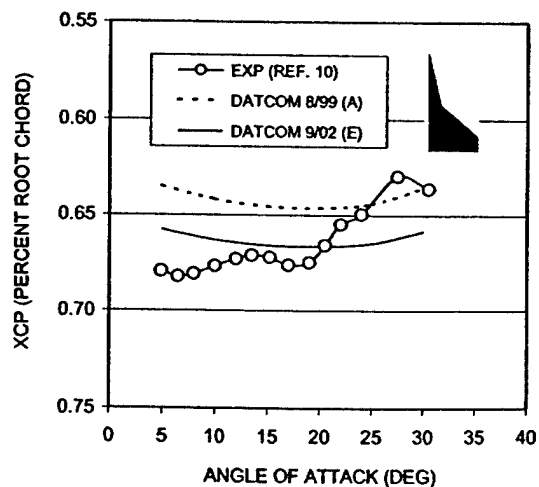


Figure 12. Wing  $x_{cp}$  Versus Angle of Attack, Configuration 22, Mach = 0.23.

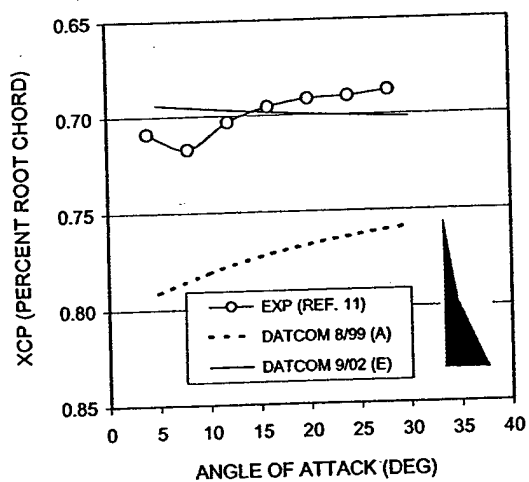


Figure 13. Wing  $x_{cp}$  Versus Angle of Attack, Configuration 23, Mach < 0.2.